

# Decoupled Action Expert: Confining Task Knowledge to the Conditioning Pathway

Jian Zhou<sup>1</sup>, Sihao Lin<sup>1</sup>, Shuai Fu<sup>1</sup>, Zerui Li<sup>1</sup>, Gengze Zhou<sup>1</sup>, Qi Wu<sup>1</sup>

**Abstract**—Many recent Vision-Language-Action models employ diffusion or flow-matching backbones with hundreds of millions of parameters for action generation. However, unlike image synthesis where the output spans millions of diverse pixels, a manipulation policy generates only short sequences of low-dimensional, physically correlated action values, a far simpler target that should not demand such capacity. We confirm this intuition and show that task-specific knowledge in these policies can be fully confined to the conditioning pathway, leaving the action backbone task-agnostic. To establish this, we introduce a decoupled training recipe: a general-purpose action head is first pretrained on observation-free forward-kinematics data, then frozen while only the conditioning pathway is trained for downstream tasks. Using Diffusion Policy as a testbed, we show that on both MimicGen and LIBERO, a single frozen backbone shared across all tasks matches normally trained counterparts. This confirms that the action expert encodes little task-specific knowledge. Ablations show that the specific pretraining signal (joint positions, end-effector poses, or no conditioning at all) has no effect on downstream performance, indicating that the backbone learns only general trajectory structure. Pushing this finding further, we replace the 244M U-Net in Diffusion Policy with a 5M-parameter MLP backbone that matches or exceeds its performance, calling into question the large capacity budgets allocated to action generation in current VLA designs.

## I. INTRODUCTION

Diffusion and flow-matching models have become one of the dominant approaches for action generation in robotic manipulation, powering both standalone Diffusion Policies [1] and the action experts within Vision-Language-Action (VLA) models such as  $\pi_0$  [2], CogACT [3], GROOT-N1 [4], and DexVLA [5]. These action experts borrow architectures from image and video generation (U-Nets, DiT blocks, flow-matching networks) along with their scale: 244M parameters for Diffusion Policy’s U-Net,  $\sim 300\text{M}$  for  $\pi_0$ ’s flow-matching network, and over 1B for DexVLA (Table I). Yet the output spaces are fundamentally different (Fig. 1). Image diffusion models denoise tens of thousands of structured latent values, while a manipulation policy generates only  $16 \times 10 = 160$  action values in Diffusion Policy [1], of which only a fraction are executed before replanning (8 steps in DP, 5 in  $\pi_0$  [2]). This orders-of-magnitude mismatch in output complexity raises a natural question: do these large action backbones actually need their capacity, or is much of it unnecessary? The question is not

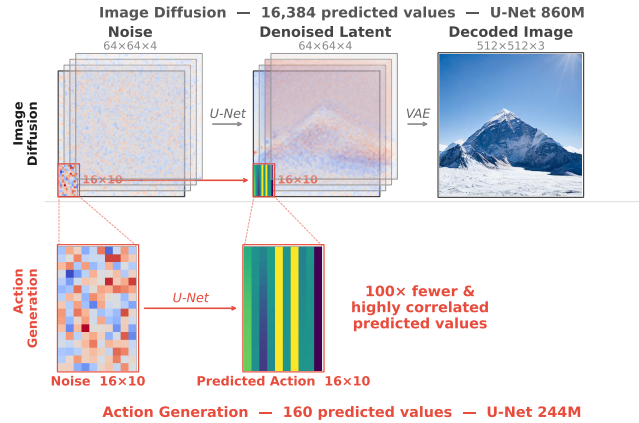


Fig. 1: Output dimensionality contrast. Image diffusion models such as Stable Diffusion [7] denoise 16,384 structured latent values, while a manipulation policy generates only 160 physically correlated values. Yet action experts in current VLA designs often adopt similar-scale architectures. Is such capacity necessary, and does the action backbone actually encode task-specific knowledge?

merely academic: recent work shows that large uninitialized action experts can destabilize VLA training through harmful gradient flows to the reasoning backbone [6], suggesting that oversized action heads are not just wasteful but actively problematic.

The problem is compounded by data scarcity: robot demonstration data is orders of magnitude smaller than what drives image or language models, making it critical to identify which policy components genuinely require task-specific demonstrations and which do not.

We investigate this through the **Decoupled Action Expert**, a two-stage training recipe that isolates the role of the action backbone:

- **Stage 1 (Observation-Free Pretraining):** A general-purpose action head is pretrained on kinematic pairs (joint positions mapped to end-effector poses via forward kinematics), available in any trajectory dataset at negligible cost, with no observation-action pairing required.
- **Stage 2 (Task-Specific Adaptation):** The pretrained action head is frozen, and only the newly initialized conditioning pathway is trained on downstream demonstrations.

The logic is straightforward: if freezing the backbone preserves task performance, then the backbone was not encoding task knowledge. Because Stage 1 requires only kinematic trajectories, the recipe can also leverage data sources that

<sup>1</sup>Jian Zhou, Sihao Lin, Shuai Fu, Zerui Li, Gengze Zhou and Qi Wu are with the Australian Institute for Machine Learning, University of Adelaide, SA, Australia. {j.zhou, sihao.lin, shuai.fu, zerui.li, gengze.zhou, qi.wu01}@adelaide.edu.au

standard observation-action pipelines cannot use at all.

Since the action expert in VLA models, such as  $\pi_0$ 's flow-matching network [2] and CogACT's DiT [3], serves the same functional role as the denoising backbone in Diffusion Policy, we use Diffusion Policy as a controlled testbed, free from confounding factors introduced by billion-parameter VLM reasoning components and tractable enough for the extensive controlled experiments across MimicGen [8] and LIBERO [9] that this study requires. Our main contributions are:

- 1) We propose the Decoupled Action Expert and use it to show that task-specific knowledge in diffusion-based policies can be confined to the conditioning pathway, leaving the action backbone task-agnostic.
- 2) We demonstrate that a 5M-parameter MLP backbone matches or exceeds a 244M-parameter U-Net, establishing that large action experts are unnecessary for robot action generation.
- 3) We show through ablation that Stage 1 conditioning type has little effect: the backbone learns general trajectory structure from any pretraining signal.
- 4) We show that the frozen backbone transfers directly from external observation-free trajectory datasets without task-specific fine-tuning.

Additionally, we identify modulation-based conditioning as the mechanism that enables decoupling, and explain why attention-based conditioning fails in this setting.

## II. RELATED WORK

Recent VLA systems predominantly generate actions through one of two paradigms: autoregressive decoding (e.g., RT-2 [10], OpenVLA [11]), or dedicated action experts that generate continuous actions via diffusion (e.g., DexVLA [5]) or flow matching (e.g.,  $\pi_0$  [2]). This paper focuses on the second paradigm. Section II-A reviews the architectures and scale of existing action experts, and Section II-B discusses the conditioning mechanisms used to steer them.

### A. Action Expert Architectures

**The  $\pi$  family and follow-up works.** The most widely adopted configuration is the  $\sim 300\text{M}$ -parameter flow-matching action expert introduced by  $\pi_0$  [2], which receives VLM features via shared self-attention and generates actions through iterative denoising. This design has been adopted by numerous subsequent works [12], [13], [14], [15], [16], [17]. Across these iterations, what changed was the conditioning interface (for example,  $\pi_{0.5}$  [12] introduced adaRMSNorm for timestep injection while retaining the shared self-attention design), but the expert's fundamental scale and role have remained fixed.

**Expert scale.** Expert capacity spans two orders of magnitude. On the compact end, CogACT [3] attaches a DiT [18] action head (13–308M) to a 7B Prismatic [19] VLM, while SmolVLA [20] and TinyVLA [21] allocate  $\sim 100\text{M}$  parameters despite aggressively compressing the VLM. At the larger end,  $\pi_{0.6}$  [22] and GR00T-N1 [4] scale to  $\sim 860\text{M}$  alongside Gemma 3 [23] 4B and Eagle-2 1.3B VLMs respectively,

TABLE I: Action expert architectures and conditioning mechanisms in recent diffusion/flow-matching policy models. Expert capacity ranges from  $\sim 100\text{M}$  in efficient VLAs [20], [21] to over 1B in DexVLA [5], yet what these backbones encode remains unexplored.

Model	Arch	Params	VLM	Conditioning
<i>Standalone (no VLM):</i>				
DP-C [1]	CNN U-Net	244M	—	FiLM
RDT-1B [28]	DiT	1.2B	—	Cross-Attn
<i><math>\sim 100\text{M}</math> experts:</i>				
CogACT [3]	DiT	13–308M	7B	Tok-Cat
SmolVLA [20]	Transformer	$\sim 100\text{M}$	350M	Cross-Attn
TinyVLA [21]	Diffusion	$\sim 100\text{M}$	0.4–1.3B	FiLM
<i><math>\sim 300\text{M}</math> experts (<math>\pi_0</math> family):</i>				
$\pi_0$ [2]	Transformer	300M	3B	Shared Self-Attn (SSA)
$\pi_{0.5}$ [12]	Transformer	300M	3B	SSA + adaRMSNorm
7+ follow-ups	Transformer	300M	3–7B	Varies
<i><math>\sim 860\text{M}</math>–1B experts:</i>				
$\pi_{0.6}$ [22]	Transformer	860M	4B	SSA + adaRMSNorm
GR00T-N1 [4]	DiT	$\sim 860\text{M}$	1.3B	Cross-Attn + AdaLN
DexVLA [5]	ScaleDP	1B	2B	FiLM + AdaLN

while DexVLA [5], PointVLA [24], GR-3 [25], and HiMoE-VLA [26] reach  $\sim 1\text{B}$  paired with 2–3B backbones [27]. CogACT's scaling studies suggest that larger action modules yield disproportionate gains [3], which may partly explain why even *efficient* VLA designs preserve substantial action experts.

Table I summarizes representative systems. Despite this architectural diversity, all dedicated action experts share the same functional role: a denoising backbone steered by a conditioning signal. Expert capacity has scaled from  $\sim 100\text{M}$  to over 1B parameters, yet the question of what these backbones actually encode (task-specific knowledge or general trajectory structure) has not been investigated. This paper provides the first such analysis.

### B. Conditioning Mechanisms

Action experts receive observation and language features through a conditioning mechanism. Existing designs fall into two structural categories that differ in where condition-specific computation resides relative to the backbone's weights.

**Attention-based conditioning** is dominant and takes three forms. Shared self-attention, pioneered by  $\pi_0$  [2] and widely adopted [13], [14], [15], [29], [30], [31], [32], [33], [17], places VLM and action tokens in a single sequence; cross-attention [4], [28], [25], [34], [35], [26], [16], [36] instead processes VLM features as external keys and values; and token concatenation [3], [37], [38], [39] prepends condition tokens to the action sequence. Despite their differences, all three route conditions through the backbone's own projections ( $W_q, W_k, W_v$ ), coupling internal representations to the conditioning distribution seen during training.

**Feature modulation** takes a structurally different approach. FiLM [40] produces per-layer scale and shift parameters ( $\gamma, \beta$ ) via a separate conditioning network, applying element-wise affine transforms to backbone features; AdaLN [18] and adaRMSNorm [12] follow the same principle through learned normalization statistics. In all cases,

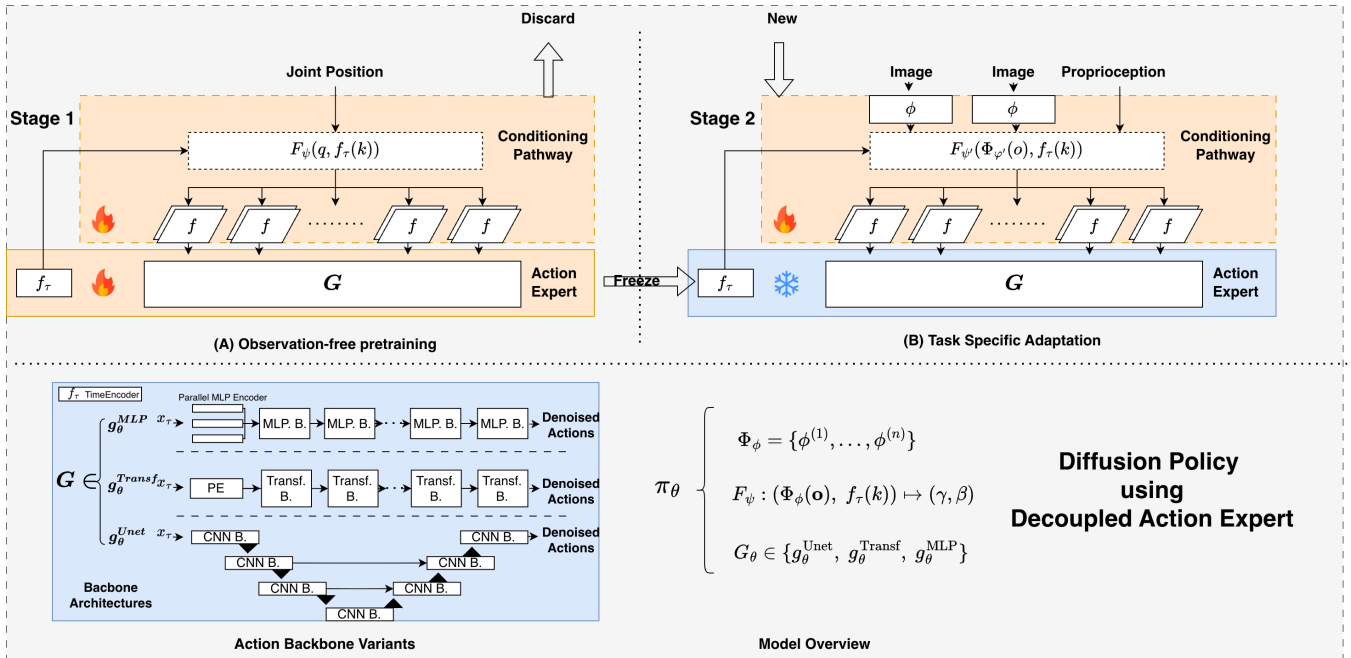


Fig. 2: Overview of Decoupled Action Expert applied to Diffusion Policy. **(A)** Stage 1 pretrains the backbone  $G_\theta$  and conditioning network  $F_\psi$  on observation-free forward-kinematics data. **(B)** Stage 2 freezes  $G_\theta$  and trains new observation encoders  $\Phi_{\phi'}$  and conditioning network  $F_{\psi'}$  on task demonstrations. Bottom left: the three backbone architectures evaluated (U-Net, Transformer, MLP). Bottom right: model overview showing the policy decomposition.

the backbone weights are condition-independent: different inputs steer the network through different operating regions via the external modulation signal. This approach is used by  $\pi_{0.5}$  [12],  $\pi_{0.6}$  [22], GROOT-N1 [4], DexVLA [5], and others [21], [41], [42].

The critical distinction is that modulation keeps all condition-specific computation in an external pathway, whereas attention-based methods distribute it across projection matrices inside the backbone. We analyze how this structural difference affects backbone reuse in Section IV-E.

### III. METHOD

If task knowledge resides in the conditioning pathway rather than the backbone, then the backbone should be (1) freezable without losing task performance and (2) replaceable with a much smaller network. We test both claims: the *Decoupled Action Expert* recipe (Section III-A) isolates the backbone by pretraining and freezing it, and *DP-MLP* (Section III-B) replaces the 244M U-Net with a 5M-parameter alternative.

#### A. Decoupled Action Expert

We decompose a FiLM-conditioned Diffusion Policy into three component groups (Fig. 2): observation encoders  $\Phi_\phi$ , a conditioning network  $F_\psi$  that produces per-layer FiLM parameters, and a denoising backbone  $G_\theta$ . The noise prediction at diffusion step  $k$  can be written as

$$\hat{\epsilon} = G_\theta(\mathbf{a}_k, F_\psi(\Phi_\phi(\mathbf{o}), f_\tau(k))), \quad (1)$$

where  $\mathbf{o}$  denotes observations,  $\mathbf{a}_k$  the noisy action sequence at diffusion step  $k$ , and  $f_\tau$  is a learned projection that

maps the diffusion timestep to a 256-dimensional embedding.  $F_\psi$  concatenates this embedding with the observation features and outputs the scale and shift parameters  $(\gamma, \beta)$  that modulate  $G_\theta$  via FiLM. The choice of FiLM conditioning is critical: because modulation keeps all condition-specific computation in the external pathway  $F_\psi$ , the backbone  $G_\theta$  remains condition-independent and can be frozen without losing the ability to represent new tasks (Section II-B). In standard training, all parameters  $\{\phi, \psi, \theta\}$  are optimized jointly on observation-action demonstrations. Our decoupled recipe separates this into two stages.

1) *Stage 1: Observation-Free Pretraining*: We exploit the deterministic forward-kinematics mapping from joint positions  $\mathbf{q}$  to end-effector poses  $\mathbf{p}$  to construct observation-free training pairs (Fig. 2, Stage 1). The backbone and conditioning network are trained to denoise end-effector pose action sequences conditioned on joint positions:

$$\hat{\epsilon} = G_\theta(\mathbf{a}_k, F_\psi(\mathbf{q}, f_\tau(k))). \quad (2)$$

Trainable parameters:  $\{\psi, \theta\}$ . No observation encoder is needed:  $\mathbf{q}$  enters the conditioning network directly. The training pairs  $(\mathbf{q}, \mathbf{p})$  can be extracted from any existing trajectory dataset at negligible cost, since joint positions and end-effector poses are standard proprioceptive signals, or generated synthetically via forward kinematics without any environment interaction.

2) *Stage 2: Task-Specific Adaptation*: The pretrained backbone  $G_\theta$  is frozen (Fig. 2, Stage 2). New observation encoders  $\Phi_{\phi'}$  and a new conditioning network  $F_{\psi'}$  are

initialized and trained on task demonstrations:

$$\hat{\epsilon} = G_{\bar{\theta}}(\mathbf{a}_k, F_{\psi'}(\Phi_{\phi'}(\mathbf{o}), f_{\tau}(k))). \quad (3)$$

Trainable parameters:  $\{\phi', \psi'\}$ . Frozen:  $\{\bar{\theta}\}$ . The observation encoder  $\Phi_{\phi'}$  is modular and can be substituted with any pretrained encoder or extended to other modalities.

### B. Lightweight Backbone: DP-MLP

The backbone  $G_{\theta}$  in DP-C is a 244M-parameter 1D convolutional U-Net [1]. A manipulation policy generates only  $16 \times 10 = 160$  action values, suggesting this capacity is unnecessary. We propose DP-MLP, which replaces the U-Net with  $L$  residual FiLM-MLP blocks totaling approximately 5M parameters ( $51 \times$  reduction). Each horizon step is embedded via a per-position linear projection, and each block applies FiLM modulation from  $F_{\psi}$  between two linear layers with a residual connection and layer normalization:

$$\mathbf{h}^{(\ell+1)} = \text{LN}(\mathbf{h}^{(\ell)} + W_2^{(\ell)}(\gamma^{(\ell)} \odot \text{GELU}(W_1^{(\ell)} \mathbf{h}^{(\ell)}) + \beta^{(\ell)})). \quad (4)$$

Because DP-MLP uses FiLM conditioning, it is directly compatible with the decoupled recipe described above. We evaluate it against the 244M U-Net in Section IV-B.

## IV. EXPERIMENTS

**Benchmarks.** We evaluate on two standard manipulation benchmarks: MimicGen [8] and LIBERO [9]. *MimicGen* extends the *robomimic* benchmark with a large set of automatically generated manipulation tasks. We select eight tasks that span coarse manipulation, fine-grained manipulation, and multi-step manipulation, each with 1000 demonstrations, and train a separate model per task. *LIBERO* [9] provides four task suites (Spatial, Object, Goal, and Long), each containing 10 language-conditioned manipulation tasks with 50 demonstrations per task. We train one model per suite. This single-task (MimicGen) and per-suite (LIBERO) protocol follows EquiDiff [43] and OpenVLA [11].

**Implementation.** On MimicGen, we adopt the original Diffusion Policy implementation [1]. Observations consist of front-view and wrist-view camera images encoded by ResNet-18, concatenated with proprioceptive state (end-effector position, quaternion orientation, and gripper openness). On LIBERO, we adopt the language-conditioned Diffusion Policy from DROID [44], which is the standard baseline used by OpenVLA [11] and subsequent works. Observations consist of front-view and wrist-view camera images encoded by ImageNet-pretrained ResNet-50, concatenated with proprioceptive state and a frozen DistilBERT [45] language embedding of the task instruction. All observation features are concatenated into a single conditioning vector that modulates the action backbone via FiLM. The DP-MLP variant is described in Section III-B. Notably, in the decoupled setting, the language embedding, like all other observation features, enters through the conditioning pathway trained in Stage 2, while the frozen backbone remains identical to the observation-free Stage 1 pretraining. Actions are 10-dimensional (3 position + 6 rotation in continuous 6D

representation [46] + 1 gripper) with a prediction horizon of 16 steps.

**Evaluation.** Unless otherwise noted, experiments are run with three random seeds (0, 42, 420) and we report mean  $\pm$  standard deviation. The conditioning mechanism ablation (Section IV-E) uses a single seed (42). On MimicGen, we evaluate every checkpoint throughout training and report the maximum success rate, following the common practice in single-task manipulation policy evaluation [43]. On LIBERO, following OpenVLA [11], we evaluate only the final checkpoint; each seed runs 500 rollouts per suite (50 per task  $\times$  10 tasks).

### A. Does Decoupling Preserve Task Performance?

The central claim of this paper is that task-specific knowledge in diffusion-based policies resides in the conditioning pathway, not the action backbone. We test this by applying the same decoupled procedure (pretrain the action backbone on observation-free kinematic data, freeze it entirely, and train only the conditioning pathway on downstream tasks) to two diffusion policy variants that differ in backbone architecture and conditioning mechanism: DP-C (U-Net, FiLM) and DP-T (transformer, cross-attention). If performance is preserved, the backbone was not encoding task knowledge. Results are shown in Table II (DP-MLP is discussed in Section IV-B).

**DP-C decoupling preserves performance.** Recall what decoupling entails: the backbone is pretrained entirely on observation-free kinematic pairs (it has never seen a single task image) and is then frozen. Only the conditioning pathway is trained on downstream demonstrations. On MimicGen, this task-blind backbone achieves  $62.2 \pm 2.3\%$  compared to  $63.6 \pm 1.8\%$  under normal training, a drop of only 1.4 points. Per-task results are mixed: decoupling slightly degrades some tasks (Stack3  $-9$ , Thread  $-8$ ) while improving others (3Piece  $+8$ , Hammer  $+4$ ), with confidence intervals largely overlapping. On LIBERO, the gap is slightly larger ( $-2.5$ :  $76.8 \pm 0.9\%$  vs.  $79.3 \pm 0.6\%$ ), concentrated in the harder Goal ( $-3.8$ ) and Long ( $-3.9$ ) suites while Spatial and Object remain within noise. This may partially stem from having fewer trainable parameters under decoupling, since the frozen backbone leaves only the conditioning layers updatable. Overall, that a frozen, task-blind backbone performs comparably to one trained end-to-end suggests that task-specific knowledge is not primarily encoded in the action backbone.

**Conditioning mechanism determines compatibility.** Not all conditioning mechanisms survive decoupling, however. DP-T, which injects observations via cross-attention, collapses from  $60.4 \pm 0.8\%$  to  $19.4 \pm 0.4\%$  on MimicGen and from  $76.4 \pm 0.4\%$  to  $5.9 \pm 0.2\%$  on LIBERO, near-total failure despite following the same decoupled procedure as DP-C. Since DP-C and DP-T differ in both backbone architecture and conditioning mechanism, this comparison alone cannot isolate the cause. We separate these two factors in Section IV-E by testing multiple conditioning mechanisms on the same backbone.

TABLE II: Normal vs. decoupled training across three architectures on MimicGen (8 tasks) and LIBERO (4 suites). FiLM-conditioned architectures DP-C (244M U-Net) and DP-MLP (5M MLP) preserve performance under decoupling, while DP-T (transformer, cross-attention) collapses (analyzed in Section IV-E). The preserved performance of a frozen, task-blind backbone indicates task knowledge resides in the conditioning pathway. The 5M MLP exceeding the 244M U-Net on both benchmarks further confirms that large action backbones are unnecessary.

		<i>MimicGen:</i>								
		Stack(A)	Square(B)	Coffee(C)	Thread(D)	Stack3(E)	Hammer(F)	3Piece(G)	Mug(H)	Avg
DP-C	Normal	100±0	55±5	73±2	47±7	95±2	54±5	17±2	67±1	63.6±1.8
	Decoupled	100±0	50±2	71±4	39±2	86±6	58±5	25±3	69±1	<b>62.2±2.3</b>
DP-T	Normal	97±1	41±2	74±6	29±2	83±7	65±2	29±3	66±2	60.4±0.8
	Decoupled	62±2	5±1	2±0	5±2	25±3	28±7	3±1	25±4	19.4±0.4
DP-MLP	Normal	100±0	51±1	76±4	47±2	89±1	61±3	36±3	69±1	<b>65.9±0.7</b>
	Decoupled	100±0	41±3	63±1	41±6	77±2	63±3	33±3	73±5	61.2±0.5

		<i>LIBERO:</i>				
		Spatial	Object	Goal	Long	Avg
DP-C	Normal	89.5±1.2	93.1±2.8	78.3±0.6	56.2±1.8	79.3±0.6
	Decoupled	87.7±1.1	92.8±1.2	74.5±1.2	52.3±2.0	76.8±0.9
DP-T	Normal	75.5±0.3	96.6±0.4	77.9±1.0	55.5±0.4	76.4±0.4
	Decoupled	4.2±1.2	8.6±1.1	8.0±0.9	2.8±0.4	5.9±0.2
DP-MLP	Normal	92.0±1.6	97.7±0.1	82.1±0.6	67.1±0.8	<b>84.7±0.5</b>
	Decoupled	87.1±1.2	98.6±0.3	82.0±1.2	68.9±1.6	<b>84.2±0.9</b>

### B. Lightweight Action Backbone

As discussed in Section II-A, action experts in recent VLA models typically range from  $\sim 100\text{M}$  to over 1B parameters, following design conventions from image diffusion models that denoise high-dimensional structured outputs: Stable Diffusion [7] produces  $64 \times 64 \times 4 = 16,384$  latent values, SDXL [47]  $128 \times 128 \times 4 = 65,536$ , and FLUX [48]  $128 \times 128 \times 16 = 262,144$ . A manipulation policy, by contrast, generates only short sequences of physically correlated, low-dimensional actions ( $16 \times 10 = 160$  values in DP, or  $50 \times 32 = 1,600$  in  $\pi_0$  [2]), two to three orders of magnitude smaller. This gap suggests that current action backbones may be heavily over-parameterized. We test this using DP-MLP (Section III-B), a 5M-parameter backbone that represents a  $51 \times$  reduction from the U-Net. Results are shown in Table II.

**A 5M MLP exceeds a 244M U-Net.** Under normal training, DP-MLP achieves  $65.9 \pm 0.7\%$  on MimicGen and  $84.7 \pm 0.5\%$  on LIBERO, both exceeding DP-C ( $63.6 \pm 1.8\%$  and  $79.3 \pm 0.6\%$ ) despite a  $51 \times$  parameter reduction. Per-task gains are especially pronounced on 3Piece (+19) and Hammer (+7) in MimicGen, and on Long (+10.9) in LIBERO, while only Stack3 (−6) trails noticeably. Under decoupling, DP-MLP retains  $61.2 \pm 0.5\%$  on MimicGen and  $84.2 \pm 0.9\%$  on LIBERO. The MimicGen decoupled drop (−4.7) is larger than DP-C’s (−1.4), driven by Coffee (−13), Stack3 (−12), and Square (−10). On LIBERO the drop is negligible (−0.5), with Goal and Long essentially unchanged and only Spatial declining (−4.9), a different pattern from DP-C, where the loss concentrated in Goal and Long. Overall, the normal training results show that a 5M MLP can exceed a 244M U-Net, while the decoupled training results further indicate that task-specific knowledge mostly does not reside in the action generation backbone.

TABLE III: Effect of pretraining data source on DP-C Decoupled.  $\Delta_N$ : difference from Normal,  $\Delta_{ID}$ : difference from In-Dist FK. DROID provides  $\sim 76\text{k}$  external Franka trajectories whose observation-free kinematics are inaccessible to standard DP training. MimicGen: mean  $\pm$  std over 3 seeds (max checkpoint). LIBERO: mean  $\pm$  std over 3 eval seeds (single training seed).

Pretrain	<i>MimicGen</i>			<i>LIBERO</i>		
	Avg	$\Delta_N$	$\Delta_{ID}$	Avg	$\Delta_N$	$\Delta_{ID}$
Normal	63.6±1.8	–	–	79.3±0.6	–	–
Dec (In-Dist FK)	62.2±2.3	−1.4	–	76.8±0.9	−2.5	–
Dec (DROID FK)	63.8±1.2	+0.2	+1.6	78.3±0.4	−1.0	+1.5

### C. Pretraining on External Trajectory Datasets

Because Stage 1 pretraining requires only observation-free kinematics, the decoupled backbone can be pretrained on any trajectory dataset containing joint-state information, a data source that standard Diffusion Policy training cannot leverage at all, since it requires paired observation–action data. We test this with DROID [44], a large-scale dataset of  $\sim 76\text{k}$  real-world Franka manipulation trajectories whose tasks and environments share no overlap with MimicGen or LIBERO. We extract only joint positions and end-effector poses, discarding all images and task labels. This also constitutes a natural data scaling experiment: in-distribution FK data is limited to the target benchmark’s own demonstrations (8,000 for MimicGen, 2,000 for LIBERO), whereas DROID contributes an order of magnitude more trajectories. Table III compares two pretraining sources: in-distribution FK and DROID FK.

DROID-pretrained backbones outperform in-distribution pretraining on both benchmarks ( $\Delta_{ID}$ : +1.6 on MimicGen, +1.5 on LIBERO), despite the complete distribution shift. This suggests that the backbone learns general kinematic structure rather than task-specific patterns, and that larger, more diverse trajectory collections can directly improve

TABLE IV: Stage 1 conditioning ablation on MimicGen (DP-C Decoupled). All variants share the same Stage 2 (freeze backbone, train new FiLM layers). Random frozen skips Stage 1 entirely. Mean  $\pm$  std over 3 seeds (max checkpoint). Task letters A–H correspond to those in Table II.

Variants	A	B	C	D
Random frozen	0 $\pm$ 0	0 $\pm$ 0	0 $\pm$ 0	0 $\pm$ 0
Unconditional ( $\emptyset \rightarrow$ eePose)	99 $\pm$ 1	53 $\pm$ 1	72 $\pm$ 0	39 $\pm$ 2
eePose self-cond (eePose $\rightarrow$ eePose)	99 $\pm$ 1	51 $\pm$ 5	74 $\pm$ 0	41 $\pm$ 3
JP conditioned (JP $\rightarrow$ eePose)	100 $\pm$ 0	50 $\pm$ 2	71 $\pm$ 4	39 $\pm$ 2

Variants	E	F	G	H	Avg
Random frozen	0 $\pm$ 0	0 $\pm$ 0	0 $\pm$ 0	0 $\pm$ 0	0.0 $\pm$ 0.0
Unconditional	85 $\pm$ 3	59 $\pm$ 3	27 $\pm$ 1	64 $\pm$ 2	62.2 $\pm$ 0.5
eePose self-cond	82 $\pm$ 2	61 $\pm$ 1	32 $\pm$ 6	69 $\pm$ 1	63.8 $\pm$ 1.1
JP conditioned	86 $\pm$ 6	58 $\pm$ 5	25 $\pm$ 3	69 $\pm$ 1	62.2 $\pm$ 2.3

the decoupled recipe, a data source entirely inaccessible to standard end-to-end training. We note that our Stage 1 pre-training is a straightforward implementation without careful design of learning rate schedules, data mixing, or curriculum. These experiments serve as an illustration that external trajectory pretraining can benefit decoupled performance, and we expect the actual gains to grow with more deliberate engineering.

#### D. Ablation: Stage 1 Conditioning

Having established that a frozen, observation-free backbone preserves task performance (Section IV-A), we now ask: what does the backbone actually learn during Stage 1, and does the choice of conditioning signal matter? We design four variants that share an identical Stage 2 procedure (freeze backbone, train new FiLM layers on MimicGen) but differ only in Stage 1. **JP conditioned** (JP  $\rightarrow$  eePose) is the standard method from Section IV-A: the backbone denoises end-effector trajectories conditioned on joint positions via forward kinematics. **Unconditional** ( $\emptyset \rightarrow$  eePose) removes all conditioning, training the backbone to denoise end-effector trajectories without any input signal. **eePose self-conditioned** (eePose  $\rightarrow$  eePose) conditions on the same end-effector trajectories, creating a trivial identity mapping. **Random frozen** skips Stage 1 entirely, freezing a randomly initialized backbone. Results are shown in Table IV.

**Pretraining is essential, but the conditioning signal is not.** The randomly initialized backbone achieves 0% across all tasks, confirming that Stage 1 pretraining is necessary for the frozen backbone to be useful. However, the three pretrained variants achieve comparable average success rates (62.2 $\pm$ 0.5%, 63.8 $\pm$ 1.1%, 62.2 $\pm$ 2.3%), with overlapping confidence intervals. Since Stage 1 FiLM layers are discarded and replaced in Stage 2, only the U-Net weights carry over, and these weights converge to a similar representation whether conditioned on joint positions, end-effector poses, or nothing at all. The backbone therefore learns general trajectory structure (temporal correlations, smooth motion priors, and end-effector geometry) regardless of the conditioning signal. This simplifies the practical requirements of the decoupled recipe: Stage 1 pretraining

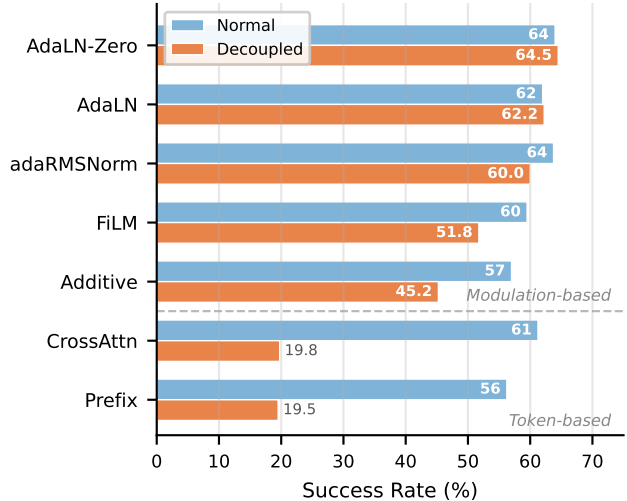


Fig. 3: Conditioning mechanism ablation on DP-T (MimicGen, seed 42). Seven mechanisms on the same transformer backbone. Under normal training all perform comparably (56–64%). Under decoupling, modulation-based methods (top) preserve performance while token-based methods (bottom) collapse.

can use any available trajectory data without requiring paired kinematic inputs.

#### E. Ablation: Conditioning Mechanism

As noted in Section IV-A, DP-C (FiLM) preserves performance under decoupling while DP-T (cross-attention) collapses, but the two architectures differ in both backbone and conditioning, leaving the root cause ambiguous. To isolate the role of the conditioning mechanism, we evaluate seven methods on the same transformer backbone ( $d=256$ , 8 layers): Cross-Attention, Prefix tuning [49], FiLM [40], AdaLN, AdaLN-Zero [18], adaRMSNorm [12], and Additive injection. Results under normal and decoupled training (seed 42) are shown in Fig. 3.

Under normal training, all seven mechanisms achieve comparable performance (56–64%), confirming that the conditioning choice does not inherently limit the backbone. Under decoupling, a clear pattern emerges based on how conditioning interacts with backbone computation. Token-based methods that embed condition-specific projections inside the backbone collapse: Cross-Attention drops from 61.3 to 19.8% and Prefix from 56.3 to 19.5%, because freezing the backbone fixes these projections to the Stage 1 input distribution. Modulation-based methods show a gradient of robustness: AdaLN-Zero and AdaLN fully preserve performance (64.0  $\rightarrow$  64.5% and 62.0  $\rightarrow$  62.3%), adaRMSNorm retains most (63.8  $\rightarrow$  60.0%), FiLM degrades moderately (59.5  $\rightarrow$  51.8%), and Additive degrades further (57.0  $\rightarrow$  45.3%). The determining factor is whether conditioning computation **separates from backbone parameters**: modulation-based methods that keep conditioning external to the backbone are robust to freezing, while token-based methods that route conditions through backbone projections collapse. Notably, several recent VLA models have independently adopted

modulation-based conditioning ( $\pi_0.5$  uses adaRMSNorm, GR00T-N1 [4] uses AdaLN, DexVLA [5] uses FiLM), consistent with our finding. All results in this ablation use a single fixed seed (42).

## V. LIMITATIONS AND FUTURE WORK

This study deliberately uses Diffusion Policy as its testbed to enable the hundreds of controlled trials and systematic ablations needed to isolate the role of the action backbone. Because VLA action experts, such as  $\pi_0$ 's flow-matching network and CogACT's DiT, serve the same functional role as the denoising backbone studied here, we expect the core findings to transfer, but directly validating the decoupled recipe on full VLA systems remains important future work. All experiments are conducted in simulation (MimicGen and LIBERO), and real-world validation is needed to confirm that the decoupled training transfers to physical manipulation. Our DROID pretraining experiments (Section IV-C) use a straightforward implementation without optimized learning rate schedules, data mixing, or curriculum. A well-designed pretraining recipe could further improve the quality of the frozen backbone, making this a promising direction for future work. Finally, since diffusion and flow-matching models call the backbone repeatedly during inference, a smaller backbone directly reduces action generation latency. We showed that a 5M MLP matches a 244M U-Net in task performance, but did not explore the minimum effective backbone size or the resulting inference speedup, both of which are worth investigating for deployment.

## REFERENCES

- [1] C. Chi, Z. Xu, S. Feng, E. Cousineau, Y. Du, B. Burchfiel, R. Tedrake, and S. Song, "Diffusion policy: Visuomotor policy learning via action diffusion," *The International Journal of Robotics Research*, 2024.
- [2] K. Black, N. Brown, D. Driess, A. Esmail, M. Equi, C. Finn, N. Fusai, L. Groom, K. Hausman, B. Ichter, S. Jakobczak, T. Jones, L. Ke, S. Levine, A. Li-Bell, M. Mothukuri, S. Nair, K. Pertsch, L. X. Shi, J. Tanner, Q. Vuong, A. Walling, H. Wang, and U. Zhilinsky, " $\pi_0$ : A vision-language-action flow model for general robot control." [Online]. Available: <http://arxiv.org/abs/2410.24164>
- [3] Q. Li, Y. Liang, Z. Wang, L. Luo, X. Chen, M. Liao, F. Wei, Y. Deng, S. Xu, Y. Zhang, X. Wang, B. Liu, J. Fu, J. Bao, D. Chen, Y. Shi, J. Yang, and B. Guo, "CogACT: A foundational vision-language-action model for synergizing cognition and action in robotic manipulation." [Online]. Available: <http://arxiv.org/abs/2411.19650>
- [4] NVIDIA, J. Bjorck, F. Castañeda, N. Cherniadev, X. Da, R. Ding, L. J. Fan, Y. Fang, D. Fox, F. Hu, S. Huang, J. Jang, Z. Jiang, J. Kautz, K. Kundalia, L. Lao, Z. Li, Z. Lin, K. Lin, G. Liu, E. Ljontop, L. Magne, A. Mandlekar, A. Narayan, S. Nasiriany, S. Reed, Y. L. Tan, G. Wang, J. Wang, J. Wang, Q. Wang, J. Xiang, Y. Xie, Y. Xu, Z. Xu, S. Ye, Z. Yu, A. Zhang, H. Zhang, Y. Zhao, R. Zheng, and Y. Zhu, "GR00t n1: An open foundation model for generalist humanoid robots." [Online]. Available: <http://arxiv.org/abs/2503.14734>
- [5] J. Wen, Y. Zhu, J. Li, Z. Tang, C. Shen, and F. Feng, "DexVLA: Vision-language model with plug-in diffusion expert for general robot control." [Online]. Available: <http://arxiv.org/abs/2502.05855>
- [6] D. Driess, J. T. Springenberg, B. Ichter, L. Yu, A. Li-Bell, K. Pertsch, A. Z. Ren, H. Walke, Q. Vuong, L. X. Shi *et al.*, "Knowledge insulating vision-language-action models: Train fast, run fast, generalize better," *arXiv preprint arXiv:2505.23705*, 2025.
- [7] R. Rombach, A. Blattmann, D. Lorenz, P. Esser, and B. Ommer, "High-resolution image synthesis with latent diffusion models," 2021.
- [8] A. Mandlekar, S. Nasiriany, B. Wen, I. Akinola, Y. Narang, L. Fan, Y. Zhu, and D. Fox, "Mimicgen: A data generation system for scalable robot learning using human demonstrations," in *7th Annual Conference on Robot Learning*, 2023.
- [9] B. Liu, Y. Zhu, C. Gao, Y. Feng, Q. Liu, Y. Zhu, and P. Stone, "Libero: Benchmarking knowledge transfer for lifelong robot learning," *Advances in Neural Information Processing Systems*, vol. 36, pp. 44 776–44 791, 2023.
- [10] A. Brohan, N. Brown, J. Carbajal, Y. Chebotar, X. Chen, K. Choromanski, T. Ding, D. Driess, A. Dubey, C. Finn, P. Florence, C. Fu, M. G. Arenas, K. Gopalakrishnan, K. Han, K. Hausman, A. Herzog, J. Hsu, B. Ichter, A. Irpan, N. Joshi, R. Julian, D. Kalashnikov, Y. Kuang, I. Leal, L. Lee, T.-W. E. Lee, S. Levine, Y. Lu, H. Michalewski, I. Mordatch, K. Pertsch, K. Rao, K. Reymann, M. Ryoo, G. Salazar, P. Sanketi, P. Sermanet, J. Singh, A. Singh, R. Soricut, H. Tran, V. Vanhoucke, Q. Vuong, A. Wahid, S. Welker, P. Wohlhart, J. Wu, F. Xia, T. Xiao, P. Xu, S. Xu, T. Yu, and B. Zitkovich, "RT-2: Vision-language-action models transfer web knowledge to robotic control." [Online]. Available: <http://arxiv.org/abs/2307.15818>
- [11] M. J. Kim, K. Pertsch, S. Karamcheti, T. Xiao, A. Balakrishna, S. Nair, R. Rafailov, E. Foster, G. Lam, P. Sanketi, Q. Vuong, T. Kollar, B. Burchfiel, R. Tedrake, D. Sadigh, S. Levine, P. Liang, and C. Finn, "OpenVLA: An open-source vision-language-action model." [Online]. Available: <http://arxiv.org/abs/2406.09246>
- [12] P. Intelligence, K. Black, N. Brown, J. Darpinian, K. Dhabalia, D. Driess, A. Esmail, M. Equi, C. Finn, N. Fusai, M. Y. Galliker, D. Ghosh, L. Groom, K. Hausman, B. Ichter, S. Jakobczak, T. Jones, L. Ke, D. LeBlanc, S. Levine, A. Li-Bell, M. Mothukuri, S. Nair, K. Pertsch, A. Z. Ren, L. X. Shi, L. Smith, J. T. Springenberg, K. Stachowicz, J. Tanner, Q. Vuong, H. Walke, A. Walling, H. Wang, L. Yu, and U. Zhilinsky, " $\pi_0.5$ : a vision-language-action model with open-world generalization." [Online]. Available: <http://arxiv.org/abs/2504.16054>
- [13] F. Lin, R. Nai, Y. Hu, J. You, J. Zhao, and Y. Gao, "OneTwoVLA: A unified vision-language-action model with adaptive reasoning." [Online]. Available: <http://arxiv.org/abs/2505.11917>
- [14] C. Fan, X. Jia, Y. Sun, Y. Wang, J. Wei, Z. Gong, X. Zhao, M. Tomizuka, X. Yang, J. Yan, and M. Ding, "Interleave-VLA: Enhancing robot manipulation with interleaved image-text instructions." [Online]. Available: <http://arxiv.org/abs/2505.02152>
- [15] T. Lin, G. Li, Y. Zhong, Y. Zou, Y. Du, J. Liu, E. Gu, and B. Zhao, "Evo-0: Vision-language-action model with implicit spatial understanding." [Online]. Available: <http://arxiv.org/abs/2507.00416>
- [16] L. Zhong, Y. Liu, Y. Wei, Z. Xiong, M. Yao, S. Liu, and G. Ren, "ACoT-VLA: Action chain-of-thought for vision-language-action models." [Online]. Available: <http://arxiv.org/abs/2601.11404>
- [17] Y. Guo, T. Lee, L. X. Shi, J. Chen, P. Liang, and C. Finn, "VLAW: Iterative co-improvement of vision-language-action policy and world model." [Online]. Available: <http://arxiv.org/abs/2602.12063>
- [18] W. Peebles and S. Xie, "Scalable diffusion models with transformers," in *Proceedings of the IEEE/CVF International Conference on Computer Vision (ICCV)*, 2023.
- [19] S. Karamcheti, S. Nair, A. Balakrishna, P. Liang, T. Kollar, and D. Sadigh, "Prismatic vlms: Investigating the design space of visually-conditioned language models," in *Forty-first International Conference on Machine Learning*, 2024.
- [20] M. Shukor, D. Aubakirova, F. Capuano, P. Kooijmans, S. Palma, A. Zouitine, M. Aractingi, C. Pascal, M. Russi, A. Marafioti, S. Alibert, M. Cord, T. Wolf, and R. Cadene, "SmolVLA: A vision-language-action model for affordable and efficient robotics." [Online]. Available: <http://arxiv.org/abs/2506.01844>
- [21] J. Wen, Y. Zhu, J. Li, M. Zhu, K. Wu, Z. Xu, N. Liu, R. Cheng, C. Shen, Y. Peng, F. Feng, and J. Tang, "TinyVLA: Towards fast, data-efficient vision-language-action models for robotic manipulation." [Online]. Available: <http://arxiv.org/abs/2409.12514>
- [22] P. Intelligence, A. Amin, R. Aniceto, A. Balakrishna, K. Black, K. Conley, G. Connors, J. Darpinian, K. Dhabalia, J. DiCarlo, D. Driess, M. Equi, A. Esmail, Y. Fang, C. Finn, C. Glossop, T. Godden, I. Goryachev, L. Groom, H. Hancock, K. Hausman, G. Hussein, B. Ichter, S. Jakobczak, R. Jen, T. Jones, B. Katz, L. Ke, C. Kuchi, M. Lamb, D. LeBlanc, S. Levine, A. Li-Bell, Y. Lu, V. Mano, M. Mothukuri, S. Nair, K. Pertsch, A. Z. Ren, C. Sharma, L. X. Shi, L. Smith, J. T. Springenberg, K. Stachowicz, W. Stoeckle, A. Swerdlow, J. Tanner, M. Torme, Q. Vuong, A. Walling,

- H. Wang, B. Williams, S. Yoo, L. Yu, U. Zhilinsky, and Z. Zhou, “ $\pi_{0,6}^*$ : a VLA that learns from experience.” [Online]. Available: <http://arxiv.org/abs/2511.14759>
- [23] G. Team, A. Kamath, J. Ferret, S. Pathak, N. Vieillard, R. Merhej, S. Perrin, T. Matejovicova, A. Ramé, M. Rivière, L. Rouillard, T. Mesnard, G. Cideron, J. bastien Grill, S. Ramos, E. Yvinec, M. Casbon, E. Pot, I. Penchev, G. Liu, F. Visin, K. Kenealy, L. Beyer, X. Zhai, A. Tsitsulin, R. Busa-Fekete, A. Feng, N. Sachdeva, B. Coleman, Y. Gao, B. Mustafa, I. Barr, E. Parisotto, D. Tian, M. Eyal, C. Cherry, J.-T. Peter, D. Sinopalnikov, S. Bhupatiraju, R. Agarwal, M. Kazemi, D. Malkin, R. Kumar, D. Vilar, I. Brusilovsky, J. Luo, A. Steiner, A. Friesen, A. Sharma, A. Sharma, A. M. Gilady, A. Goedeckemeyer, A. Saade, A. Feng, A. Kolesnikov, A. Bendebury, A. Abdagic, A. Vadi, A. György, A. S. Pinto, A. Das, A. Bapna, A. Miech, A. Yang, A. Paterson, A. Shenoy, A. Chakrabarti, B. Piot, B. Wu, B. Shahriari, B. Petrini, C. Chen, C. L. Lan, C. A. Choquette-Choo, C. Carey, C. Brick, D. Deutsch, D. Eisenbud, D. Cattle, D. Cheng, D. Paparas, D. S. Sreepathihalli, D. Reid, D. Tran, D. Zelle, E. Noland, E. Huizenga, E. Khaitonov, F. Liu, G. Amirkhanyan, G. Cameron, H. Hashemi, H. Klimczak-Plucińska, H. Singh, H. Mehta, H. T. Lehri, H. Hazimeh, I. Ballantyne, I. Szepkovi, I. Nardini, J. Pouget-Abadie, J. Chan, J. Stanton, J. Wieting, J. Lai, J. Orbay, J. Fernandez, J. Newlan, J. yeong Ji, J. Singh, K. Black, K. Yu, K. Hui, K. Vodrahalli, K. Greff, L. Qiu, M. Valentine, M. Coelho, M. Ritter, M. Hoffman, M. Watson, M. Chaturvedi, M. Moynihan, M. Ma, N. Babar, N. Noy, N. Byrd, N. Roy, N. Momchev, N. Chauhan, N. Sachdeva, O. Bunyan, P. Botarda, P. Caron, P. K. Rubenstein, P. Culliton, P. Schmid, P. G. Sessa, P. Xu, P. Stanczyk, P. Tafti, R. Shivanna, R. Wu, R. Pan, R. Rokni, R. Willoughby, R. Vallu, R. Mullins, S. Jerome, S. Smoot, S. Girgin, S. Iqbal, S. Reddy, S. Sheth, S. Pöder, S. Bhatnagar, S. R. Panyam, S. Eiger, S. Zhang, T. Liu, T. Yacovone, T. Liechty, U. Kalra, U. Evcı, V. Misra, V. Roseberry, V. Feinberg, V. Kolesnikov, W. Han, W. Kwon, X. Chen, Y. Chow, Y. Zhu, Z. Wei, Z. Egyed, V. Cotruta, M. Giang, P. Kirk, A. Rao, K. Black, N. Babar, J. Lo, E. Moreira, L. G. Martins, O. Sanseviero, L. Gonzalez, Z. Gleicher, T. Warkentin, V. Mirrokni, E. Senter, E. Collins, J. Barral, Z. Ghahramani, R. Hadsell, Y. Matias, D. Sculley, S. Petrov, N. Fiedel, N. Shazeer, O. Vinyals, J. Dean, D. Hassabis, K. Kavukcuoglu, C. Farabet, E. Buchatskaya, J.-B. Alayrac, R. Anil, Dmitry, Lepikhin, S. Borgeaud, O. Bachem, A. Joulin, A. Andreev, C. Hardin, R. Dadashi, and L. Hussenot, “Gemma 3 technical report,” 2025. [Online]. Available: <https://arxiv.org/abs/2503.19786>
- [24] C. Li, J. Wen, Y. Peng, Y. Peng, F. Feng, and Y. Zhu, “PointVLA: Injecting the 3d world into vision-language-action models.” [Online]. Available: <http://arxiv.org/abs/2503.07511>
- [25] C. Cheang, S. Chen, Z. Cui, Y. Hu, L. Huang, T. Kong, H. Li, Y. Li, Y. Liu, X. Ma, H. Niu, W. Ou, W. Peng, Z. Ren, H. Shi, J. Tian, H. Wu, X. Xiao, Y. Xiao, J. Xu, and Y. Yang, “GR-3 technical report.” [Online]. Available: <http://arxiv.org/abs/2507.15493>
- [26] Z. Du, B. Liu, Y. Liang, Y. Shen, H. Cao, X. Zheng, Z. Feng, Z. Wu, J. Yang, and Y.-G. Jiang, “HiMoE-VLA: Hierarchical mixture-of-experts for generalist vision-language-action policies.” [Online]. Available: <http://arxiv.org/abs/2512.05693>
- [27] P. Wang, S. Bai, S. Tan, S. Wang, Z. Fan, J. Bai, K. Chen, X. Liu, J. Wang, W. Ge *et al.*, “Qwen2-vl: Enhancing vision-language model’s perception of the world at any resolution,” *arXiv preprint arXiv:2409.12191*, 2024.
- [28] S. Liu, L. Wu, B. Li, H. Tan, H. Chen, Z. Wang, K. Xu, H. Su, and J. Zhu, “RDT-1b: a diffusion foundation model for bimanual manipulation.” [Online]. Available: <http://arxiv.org/abs/2410.07864>
- [29] H. Huang, M. Cen, K. Tan, X. Quan, G. Huang, and H. Zhang, “GraphCoT-VLA: A 3d spatial-aware reasoning vision-language-action model for robotic manipulation with ambiguous instructions.” [Online]. Available: <http://arxiv.org/abs/2508.07650>
- [30] G. Yang, T. Zhang, H. Hao, W. Wang, Y. Liu, D. Wang, G. Chen, Z. Cai, J. Chen, W. Su, W. Zhou, Y. Qiao, J. Dai, J. Pang, G. Luo, W. Wang, Y. Mu, and Z. Hou, “Vlaser: Vision-language-action model with synergistic embodied reasoning.” [Online]. Available: <http://arxiv.org/abs/2510.11027>
- [31] S. Fan, K. Wu, Z. Che, X. Wang, D. Wu, F. Liao, N. Liu, Y. Zhang, Z. Zhao, Z. Xu, M. Li, Q. Liu, S. Zhang, M. Wan, and J. Tang, “XR-1: Towards versatile vision-language-action models via learning unified vision-motion representations.” [Online]. Available: <http://arxiv.org/abs/2511.02776>
- [32] W. Wu, F. Lu, Y. Wang, S. Yang, S. Liu, F. Wang, Q. Zhu, H. Sun, Y. Wang, S. Ma, Y. Ren, K. Zhang, H. Yu, J. Zhao, S. Zhou, Z. Qiu, H. Xiong, Z. Wang, Z. Wang, R. Cheng, Y.-L. Li, Y. Huang, X. Zhu, Y. Shen, and K. Zheng, “A pragmatic VLA foundation model.” [Online]. Available: <http://arxiv.org/abs/2601.18692>
- [33] G. Team, A. Ye, B. Wang, C. Ni, G. Huang, G. Zhao, H. Li, J. Li, J. Zhu, L. Feng, P. Li, Q. Deng, R. Ouyang, W. Qin, X. Chen, X. Wang, Y. Wang, Y. Li, Y. Li, Y. Ding, Y. Xu, Y. Ye, Y. Zhou, Z. Dong, Z. Wang, Z. Liu, and Z. Zhu, “GigaBrain-0: A world model-powered vision-language-action model.” [Online]. Available: <http://arxiv.org/abs/2510.19430>
- [34] M. Reuss, H. Zhou, M. Rühle, Ö. E. Yağmurlu, F. Otto, and R. Lioutikov, “FLOWER: Democratizing generalist robot policies with efficient vision-language-action flow policies.” [Online]. Available: <http://arxiv.org/abs/2509.04996>
- [35] H. Shi, B. Xie, Y. Liu, L. Sun, F. Liu, T. Wang, E. Zhou, H. Fan, X. Zhang, and G. Huang, “MemoryVLA: Perceptual-cognitive memory in vision-language-action models for robotic manipulation.” [Online]. Available: <http://arxiv.org/abs/2508.19236>
- [36] S. Deng, M. Yan, S. Wei, H. Ma, Y. Yang, J. Chen, Z. Zhang, T. Yang, X. Zhang, W. Zhang, H. Cui, Z. Zhang, and H. Wang, “GraspVLA: a grasping foundation model pre-trained on billion-scale synthetic action data.” [Online]. Available: <http://arxiv.org/abs/2505.03233>
- [37] O. M. Team, D. Ghosh, H. Walke, K. Pertsch, K. Black, O. Mees, S. Dasari, J. Hejna, T. Kreiman, C. Xu, J. Luo, Y. L. Tan, L. Y. Chen, P. Sanketi, Q. Vuong, T. Xiao, D. Sadigh, C. Finn, and S. Levine, “Octo: An open-source generalist robot policy.” [Online]. Available: <http://arxiv.org/abs/2405.12213>
- [38] S. Lian, B. Yu, X. Lin, L. T. Yang, Z. Shen, C. Wu, Y. Miao, C. Huang, and K. Chen, “LangForce: Bayesian decomposition of vision language action models via latent action queries.” [Online]. Available: <http://arxiv.org/abs/2601.15197>
- [39] J. Sun, W. Zhang, Z. Qi, S. Ren, Z. Liu, H. Zhu, G. Sun, X. Jin, and Z. Chen, “VLA-JEPA: Enhancing vision-language-action model with latent world model.” [Online]. Available: <http://arxiv.org/abs/2602.10098>
- [40] E. Perez, F. Strub, H. de Vries, V. Dumoulin, and A. Courville, “FiLM: Visual reasoning with a general conditioning layer,” in *Proceedings of the AAAI Conference on Artificial Intelligence*, 2018.
- [41] J. Li, Y. Zhu, Z. Tang, J. Wen, M. Zhu, X. Liu, C. Li, R. Cheng, Y. Peng, Y. Peng, and F. Feng, “CoA-VLA: Improving vision-language-action models via visual-textual chain-of-affordance.” [Online]. Available: <http://arxiv.org/abs/2412.20451>
- [42] J. Wen, M. Zhu, Y. Zhu, Z. Tang, J. Li, Z. Zhou, C. Li, X. Liu, Y. Peng, C. Shen, and F. Feng, “Diffusion-VLA: Generalizable and interpretable robot foundation model via self-generated reasoning.” [Online]. Available: <http://arxiv.org/abs/2412.03293>
- [43] D. Wang, S. Hart, D. Surovik, T. Kelestemur, H. Huang, H. Zhao, M. Yeatman, J. Wang, R. Walters, and R. Platt, “Equivariant diffusion policy,” 2024. [Online]. Available: <https://arxiv.org/abs/2407.01812>
- [44] A. Khazatsky, K. Pertsch, S. Nair, A. Balakrishna, S. Dasari, S. Karamcheti, S. Nasiriany, M. K. Srirama, L. Y. Chen, K. Ellis *et al.*, “Droid: A large-scale in-the-wild robot manipulation dataset,” *arXiv preprint arXiv:2403.12945*, 2024.
- [45] V. Sanh, L. Debut, J. Chaumond, and T. Wolf, “Distilbert, a distilled version of bert: smaller, faster, cheaper and lighter,” *arXiv preprint arXiv:1910.01108*, 2019.
- [46] Y. Zhou, C. Barnes, J. Lu, J. Yang, and H. Li, “On the continuity of rotation representations in neural networks,” in *Proceedings of the IEEE/CVF conference on computer vision and pattern recognition*, 2019, pp. 5745–5753.
- [47] D. Podell, Z. English, K. Lacey, A. Blattmann, T. Dockhorn, J. Müller, J. Penna, and R. Rombach, “Sdxl: Improving latent diffusion models for high-resolution image synthesis,” *arXiv preprint arXiv:2307.01952*, 2023.
- [48] B. F. Labs, S. Batifol, A. Blattmann, F. Boesel, S. Consul, C. Diagne, T. Dockhorn, J. English, Z. English, P. Esser *et al.*, “Flux. 1 kontext: Flow matching for in-context image generation and editing in latent space,” *arXiv preprint arXiv:2506.15742*, 2025.
- [49] X. L. Li and P. Liang, “Prefix-tuning: Optimizing continuous prompts for generation,” in *Proceedings of the 59th Annual Meeting of the Association for Computational Linguistics and the 11th International Joint Conference on Natural Language Processing (Volume 1: Long Papers)*, 2021, pp. 4582–4597.